

of nonlinear terms which may become increasingly important in more advanced demixed states. Equations III-19 and III-24 indicate, respectively, that the concentration fluctuations completely disappear and that the scattered intensity goes to zero after a sufficient period of time. This is not correct, because there are thermal fluctuations even in homogeneous mixtures which causes elastic scattering equal to $I_H(q; T_x)$. A correction for this effect was made in eq V-2 and the corrected scattered intensity $I_{\text{corr}}(q, t)$ was compared with $I_{\text{theor}}(q, t)$ in eq III-24. A more rigorous theoretical treatment is obviously required, and the theory should allow $I_{\text{theor}}(q, t)$ to approach $I_H(q; T_x)$ at $t \rightarrow \infty$ by properly accounting for the thermal noise appropriate to the small- q regime.

Registry No. PS (homopolymer), 9003-53-6; PVME (homopolymer), 9003-09-2.

References and Notes

- (1) van Aartsen, J. J. *Eur. Polym. J.* **1970**, *6*, 919.
- (2) van Aartsen, J. J.; Smolders, C. A. *Eur. Polym. J.* **1970**, *6*, 1105.
- (3) Nishi, T.; Wang, T. T.; Kwei, T. K. *Macromolecules* **1975**, *8*, 227.
- (4) de Gennes, P.-G. *J. Chem. Phys.* **1980**, *72*, 4756.
- (5) Pincus, P. J. *J. Chem. Phys.* **1981**, *75*, 1996.
- (6) Nojima, S.; Tsutsumi, T.; Nose, T. *Polym. J.* **1982**, *14*, 225.
- (7) Nojima, S.; Ohyama, Y.; Yamaguchi, M.; Nose, T. *Polym. J.* **1982**, *14*, 907.
- (8) Hashimoto, T.; Kumaki, J.; Kawai, H. *Macromolecules* **1983**, *16*, 641.
- (9) Snyder, H. L.; Meakin, P.; Reich, S. *Macromolecules* **1983**, *16*, 757.
- (10) Gelles, R.; Frank, C. W. *Macromolecules* **1983**, *16*, 1448.
- (11) Snyder, H. L.; Meakin, P. *J. Chem. Phys.* **1983**, *79*, 5588.
- (12) Binder, K. *J. Chem. Phys.* **1983**, *79*, 6387.
- (13) Hashimoto, T.; Sasaki, K.; Kawai, H. *Macromolecules* **1984**, *17*, 2812.
- (14) Sasaki, K.; Hashimoto, T. *Macromolecules* **1984**, *17*, 2818.
- (15) Inoue, T.; Ougizawa, T.; Yasuda, O.; Miyasaka, K. *Macromolecules* **1985**, *18*, 57.
- (16) Russell, T. P.; Hadziioannou, G.; Warburton, W. K. *Macromolecules* **1985**, *18*, 78.
- (17) Strobl, G. R. *Macromolecules* **1985**, *18*, 558.
- (18) Bank, M.; Leffingwell, J.; Thies, C. *Macromolecules* **1971**, *4*, 43; *J. Polym. Sci., Polym. Phys. Ed.* **1972**, *10*, 1097.
- (19) Nishi, T.; Kwei, T. K. *Polymer* **1975**, *16*, 285.
- (20) Tanaka, K.; Saijo, K.; Suehiro, S.; Hashimoto, T.; Kawai, H. *Polym. Prepr. Jpn.* **1981**, *30*, 2094.
- (21) Flory, P. "Principles of Polymer Chemistry", Cornell University Press: Ithaca, NY, 1971.
- (22) Cahn, J. W.; Hilliard, J. E. *J. Chem. Phys.* **1958**, *29*, 258; **1959**, *31*, 688.
- (23) Cahn, J. W. *J. Chem. Phys.* **1965**, *42*, 93.
- (24) This restriction is reasonable since the q region covered by this light scattering method is $q < 10^5 \text{ cm}^{-1}$ and R_0 is the order of 10^{-6} cm and hence $qR_0 < 10^{-1}$.
- (25) Izumitani, T.; Hashimoto, T. *J. Chem. Phys.* **1985**, *83*, 3694.
- (26) The demixing in the unstable region for this particular mixture definitely involves the exponential growth of the scattered intensity with time over a sufficiently long time interval, and this time interval increases with decreasing quench depth. Hence the nonexponential growth observed at temperatures 106 and 104 °C, lower than $T_c = 107$ °C, i.e., at smaller quench depths, can be best interpreted as a manifestation of the nucleation and growth.
- (27) Recent experiments of Shelten et al.²⁸ and Stein et al.²⁹ have shown that χ is a function of ϕ .
- (28) Herkt-Maetzky, C.; Schelten, J. *Phys. Rev. Lett.* **1983**, *51*, 896.
- (29) Yang, H.; Shibayama, M.; Stein, R. S.; Han, C. C. *Polym. Bull.* **1984**, *12*, 7. Shibayama, M.; Yang, H.; Stein, R. S.; Han, C. C. *Macromolecules* **1985**, *18*, 2179.
- (30) The gradient free energy appearing on the right-hand side of eq III-11 originates from nonlocal entropic contributions to F rather than nonlocal energetic contributions. The nonlocal energetic contributions were neglected as they are small compared with the entropic contributions associated with connectivity of the segments. The nonlocal entropy contributions for polymer solutions were described by Vrij and van den Esker.³¹
- (31) Vrij, A.; van den Esker, M. W. J. *J. Chem. Soc., Faraday Trans. 2* **1972**, *68*, 513.

Static Light Scattering Study of High Molecular Weight 18-Arm Star Block Copolymers

Anh B. Nguyen,^{1a} Nikos Hadjichristidis,^{1b} and Lewis J. Fetters^{*1c}

Institute of Polymer Science, University of Akron, Akron, Ohio 44325.

Received August 23, 1985

ABSTRACT: Light scattering studies on very high molecular weight 18-arm star poly(styrene-isoprene) block copolymers have been done by using, in part, isorefractive solvents. The radius of gyration of the polystyrene outer blocks is expanded to approximately the same size as the whole macromolecule while that of the polyisoprene inner segment assumes the dimensions of a homopolyisoprene star of equivalent molecular weight and functionality. The shape of the polystyrene outer blocks resembles that predicted for a hollow star. The findings support the presence of a segregated vesicle-like conformation in dilute solution.

Introduction

The dilute solution conformational aspects of linear di- or triblock copolymers have been the subject of experimental²⁻¹³ and theoretical¹⁴⁻¹⁶ considerations. The architecture of copolymers containing homopolymer segments can influence their dilute solution conformation. An example of this behavior is seen in the model graft copolymer work of Rahlwes, Roovers, and Bywater¹⁷ and Hadjichristidis and Roovers.¹⁸ The latter authors, via the use of isorefractive solvents, reached the conclusion that intramolecular separation existed and that the conformation of the poly(isoprene-*g*-styrene) copolymer could be classified as a core-shell structure in dilute solution with the polyisoprene backbone preferentially occupying the

core. In view of this latter result, it is apparent that the conformation of a star block copolymer could be studied in a similar fashion by measuring the apparent radii of gyration in isorefractive solvents. Furthermore, because of the anticipated "advantageous" geometry of star block copolymers, their conformation would be expected to be amenable to a shape analysis by an evaluation of the particle scattering factor. This dual approach applied to two high molecular weight 18-arm star block copolymers is the subject of this paper.

Experimental Section

Two high molecular weight star block copolymer materials were prepared in benzene. Dilute solutions, $\approx 2\%$ (w/v), were adhered to in the polymerizations. The linking reaction, involving an

Table I
Molecular Characteristics of Poly(styrene-isoprene)
18-Arm Star Block Copolymers

sample	wt % polystyrene ^a	type	$\bar{M}_n \times 10^{-6}^b$	$\bar{M}_w \times 10^{-6}$	f_w^c
18/46/152	0.46	arm	0.325	0.330 ^d	
		star	5.85	5.82	17.6
18/23/154	0.23	arm	0.663	0.670 ^e	
		star	11.9	11.5	17.2

^a Via ¹H NMR. ^b Predicted (stoichiometric) number-average molecular weight. ^c $f_w = \bar{M}_w(\text{star})/\bar{M}_w(\text{arm})$. ^d Segment molecular weights: PS = 1.52×10^5 ; PI = 1.78×10^5 . ^e Segment molecular weights: PS = 1.54×10^5 ; PI = 5.16×10^5 .

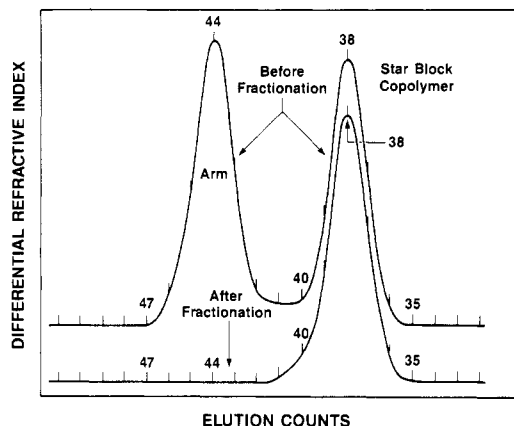


Figure 1. Size exclusion chromatographs of unfractionated and fractionated 18/46/152 star block copolymer (1 count = 5 mL).

octadecachlorosilane,¹⁹⁻²¹ was allowed to proceed for 3 weeks at ca. 20 °C followed by 1 week at 40 °C prior to termination of the residual active centers. The amount of reactive sites of the linking agent was about 50% of the active center concentration. This was done in order to enhance the extent of reaction. The fractionation of the unlinked block copolymer arms from the star branched polymer was done by using a 1:1 (v/v) toluene/cyclohexane mixture containing 0.2% (w/v) of block copolymer. Methanol was the nonsolvent. Three to four fractionations were needed in order to obtain essentially pure star block copolymer. The polyisoprene segment was found, via ¹H NMR, to have the anticipated >90% 1,4 mode of concatenation (cis/trans ≈ 8/2).

Six different solvents were used for the light scattering experiments. Toluene, cyclohexane, and chlorobenzene were purified by refluxing for 1 to 2 days over calcium hydride before distillation. Tetrahydrofuran and dioxane were purified following the procedure of Hadjichristidis and Roovers.¹⁸ Bromoform was washed with water, dried over K₂CO₃, and distilled at low pressure (ca. 10 mmHg) taking only the middle cut. Diphenylamine was added as the stabilizer (~0.01% w/v). All of the solvents were distilled on the day the polymer solutions were prepared. Special care was given to shield bromoform from light prior to the measurements.

A Brice-Phoenix differential refractometer was used for the dn/dc measurements at 436 nm. The light scattering measurements were accomplished by using the Sofica PGD instrument with unpolarized light at 436 nm at 35 °C. The scattering intensities were measured over the angular range of 30–150°. The solutions were clarified for 1 h by centrifugation at 1.4×10^4 rpm. Size exclusion chromatography measurements were done with a Waters Ana-Prep instrument equipped with a seven-column Styragel set. An operation temperature of 30 °C was maintained with tetrahydrofuran as the mobile phase at a flow rate of 1 mL min⁻¹.

Results

Table I contains the molecular characteristics of the two star block copolymer samples. The experimental functionality was taken as the ratio of $\bar{M}_w(\text{star})/\bar{M}_w(\text{arm})$ since the more appropriate $\bar{M}_n(\text{star})$ values were inaccessible.

Table II
Refractive Index Increments dn/dc (mL g⁻¹) at 436 nm and 35 °C

THF	toluene	chloro- benzene	bromoform	cyclo- hexane	dioxane
polystyrene					
0.208 ^a	0.117	0.084 ^a	0.010 ^a	0.181 ^a	0.189
polyisoprene					
0.148 ^a	0.027	-0.004 ^a	-0.082 ^a	0.117 ^a	0.114
18/46/152 ^b					
0.175	0.067	0.036	-0.043	0.149	0.149
0.176	0.068	0.036	-0.040	0.146	0.149
18/23/154 ^b					
0.159	0.049	0.017	-0.067	0.135	0.131
0.162	0.048	0.019	-0.061	0.132	0.131

^a Literature values (ref 8 and 17). ^b First line lists experimental values and the second line the calculated ones.

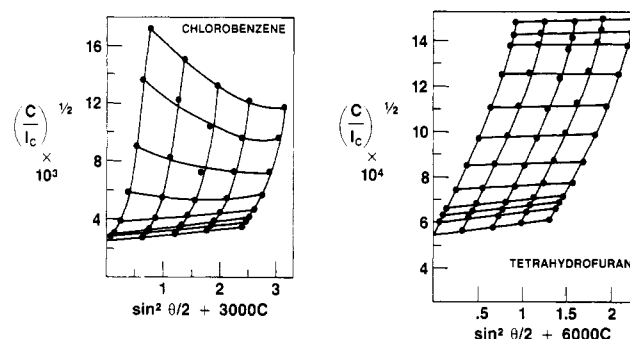


Figure 2. Zimm-Berry plots of the 18/46/152 star block copolymer.

The fact that essentially pure star block copolymers were obtained following fractionation is illustrated in Figure 1.

The dn/dc values of the star block copolymers and the linear homopolymers are shown in Table II. The experimental values can be compared to the values calculated from the following relation:²²

$$dn/dc = x(dn/dc)_A + (1-x)(dn/dc)_B$$

where x is the fraction of homopolymer A in the AB star block copolymer. Within the limits of experimental error the experimental and calculated dn/dc values are identical. The experimental values were used in this work.

The Zimm plots for the star block copolymers exhibited varying degrees of curvature for the results in all six solvents. Thus, in order to obtain reliable extrapolations, the data were handled by using Berry's method.²³ Representative Zimm-Berry plots are shown in Figure 2. Previous observations have shown that curved Zimm⁸ and Zimm-Berry¹⁷ plots (similar to that of Figure 2) are obtained when the refractive index of either component approaches that of the solvent for linear diblock or graft copolymer systems having molecular weights, \bar{M}_w , greater than 8×10^5 . This distortion apparently arises as a consequence of intermolecular interference effects resulting from the large abnormal excluded volume for the visible portion of the copolymer. Conversely, though, distortion was absent in the Zimm-Berry plots obtained¹⁸ in chlorobenzene and bromoform of a poly(isoprene-*g*-styrene) graft copolymer having an \bar{M}_w of 1.2×10^6 . Thus, the overall molecular weight, the composition, the component molecular weights, and the architecture of these segmented copolymers seemingly influence the extent of intermolecular interference observed.

Tables III and IV list the *apparent* weight-average molecular weights and mean-square radii of gyration for

Table III
Molecular Weights and Chain Dimensions for 18/46/152
Star Block Copolymer in Various Solvents

solvent	$\bar{M}_w \times 10^{-6}$	$\langle S^2 \rangle \times 10^{11},$ cm ²
tetrahydrofuran	5.46	5.47
toluene	5.96	5.33
chlorobenzene ^a	6.02	5.18
bromoform ^b	5.93	1.94
cyclohexane	5.91	4.36
dioxane	5.63	2.70

^a Isorefractive with polyisoprene. ^b Isorefractive with polystyrene.

Table IV
Molecular Weights and Chain Dimensions for 18/23/154
Star Block Copolymer in Various Solvents

solvent	$\bar{M}_w \times 10^{-6}$	$\langle S^2 \rangle \times 10^{11},$ cm ²
tetrahydrofuran	10.9	14.4
toluene	12.0	16.9
chlorobenzene ^a	12.0	
bromoform ^b	13.0	9.0
cyclohexane	11.6	11.1
dioxane	9.4	8.1

^a Isorefractive with polyisoprene. ^b Isorefractive with polystyrene.

the two star block copolymers 18/46/152 and 18/23/154. The fairly constant molecular weights found in the various solvents for the two materials are indicative of the high degree of homogeneity in molecular weight and composition of these samples.

Particle Scattering Factor $P(\theta)$. When the dimension of a scattering particle is larger than $\lambda/20$ (where λ is the wavelength of light), the intensity of the light scattered at an angle θ is attenuated because of destructive interference.²⁴ This effect, designated by $P(\theta)$, is dependent on the angle of observation and on the size and shape of the particle. For these reasons $P(\theta)$ is referred to as the particle scattering factor, or the form factor, and is defined as follows:

$$P(\theta) = i_\theta / i_{\theta=0} = R_\theta / R_{\theta=0}$$

where i_θ and R_θ are the intensity and the Rayleigh ratio at θ angle, respectively. A quantitative evaluation of this effect was first given by Debye²⁵ for polymers in dilute solution

$$P(\theta) = \frac{1}{N^2} \sum_{i=1}^N \sum_{j=1}^N \left\langle \frac{\sin hr_{ij}}{r_{ij}} \right\rangle$$

where N is the number of scattering points, r_{ij} the distance between two scattering points, and $h = (4\pi/\lambda) \sin(\theta/2)$, also known as the scattering vector. Only purely geometrical quantities appear in this expression. Generally $P^{-1}(\theta)$ is plotted against u^2 , where $u^2 = [(4\pi/\lambda) \sin(\theta/2)]^2 \langle S^2 \rangle$. It is interesting to note that in order for an experimental study on the shape of a polymer to be meaningful one has to work at high u^2 . This can be achieved by either a larger $\langle S^2 \rangle$ or a very low λ . Thus, very high molecular weight materials were used in this study. $P(\theta)$ can be quantitatively evaluated for a wide variety of species of varying architecture. Theoretical studies^{11,26} show that as a homostar grows in arms of equal length, its $P(\theta)$ undergoes a rapid upturn with increasing u^2 .

In 1970, Kajiwara et al.²⁶ showed that the statistical cascade theory of branching processes was useful for the $P(\theta)$ analysis of randomly branched copolymers. In 1974,

Burchard²⁷ extended the cascade theory to cover the case of polymeric stars with particular attention given to the $P(\theta)$ factor. The equations for $P(\theta)$, or more exactly $P(h)$ since h is a function of θ , were given as^{28,29}

$$P(h) = \frac{2}{f u^2} [v - (1 - \exp(-v))] + \frac{f-1}{2} [1 - \exp(-v)^2]$$

(monodisperse arms following Gaussian statistics), where $v = [f/(3f-2)]u^2$ and f is a functionality, and

$$P(h) = \frac{1 + u^2/3f}{(1 + u^2(f+1)/6f)^2}$$

(polydisperse arms with most probable distribution). Burchard²⁷ also calculated the $P(h)$ of a copolymeric star of different specific refractive indices. When $\nu_A = \nu_B$ the copolymer star becomes, in effect, a homostar. Of particular interest is when the solvent is isorefractive with the center block $\nu_B = 0$; then, in Burchard's terminology, a "ghost star"²⁷ is formed with the arms seemingly grafted to an invisible core. Burchard stated that the branching effect can be seen more easily in a plot of $P(h)u^2$ vs. u , often called the Kratky plot. A Kratky plot can differentiate the functionality of a star by the sharpness and the position of its maximum. Hence the shape of the star-shaped block copolymer, and therefore its conformation in non-isorefractive and isorefractive solvents, can be directly compared to the $P(h)$ function evaluated for star models of varying functionalities and varying specific refractive index increment values.

Discussion

Since the (dn/dc) values of polystyrene and polyisoprene in tetrahydrofuran, toluene, cyclohexane, and dioxane are high and positive (Table II), it is possible, to a first approximation, to make a comparison among the $\langle S^2 \rangle$ values measured in those solvents. The $\langle S^2 \rangle$ values measured in tetrahydrofuran and toluene are 5.47×10^{-11} and 5.33×10^{-11} cm², respectively, for 18/46/152. Both are good solvents for polystyrene and polyisoprene. However, the values of $\langle S^2 \rangle$ are lower in cyclohexane (4.36×10^{-11} cm²) and in dioxane (2.70×10^{-11} cm²). This reduction in $\langle S^2 \rangle$ is caused by the selective solvent nature of cyclohexane and dioxane; i.e., at 35 °C cyclohexane is a θ solvent for polystyrene and dioxane is a near- θ solvent for polyisoprene. Consequently, the contractions of the polystyrene blocks and the polyisoprene blocks to their quasi-unperturbed dimensions in cyclohexane and dioxane, respectively, are responsible for the lowered values of $\langle S^2 \rangle$ in these solvents.

The values of $\langle S^2 \rangle$ measured in the two isorefractive solvents (chlorobenzene and bromoform) are of particular interest. The $\langle S^2 \rangle$ measured in chlorobenzene (5.18×10^{-11} cm²) is very close to the true $\langle S^2 \rangle$ of the 18/46/152 star block copolymer. Likewise the value obtained in the bromoform (1.94×10^{-11} cm²) is almost equivalent to the true $\langle S^2 \rangle$ of the polyisoprene blocks.³⁰ Thus the dimensions exhibited by the polystyrene portion is larger than that of the polyisoprene fraction. Expressed in angstrom units, the apparent radii of gyration of the polystyrene "ghost star" and polyisoprene core are 720 and 440 Å, respectively. This large expansion in the dimensions of the polystyrene blocks in a sample having 46% of polystyrene strongly suggests that this 18-armed star block copolymer assumes a segregated conformation with the polyisoprene blocks residing in the core with the polystyrene segments forming the shell.

The very high molecular weight of the 18/23/154 star block copolymer made it difficult to obtain accurate

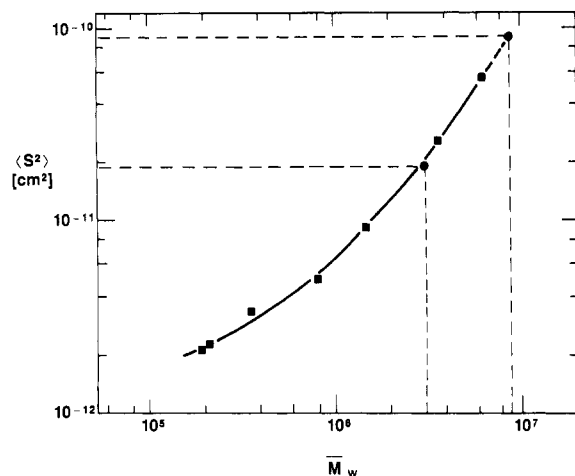


Figure 3. Radii of gyration of 18-arm polyisoprene stars (squares) in cyclohexane at 35 °C. Circles represent the apparent radii of gyration of the polyisoprene portion of the 18/46/152 and 18/23/154 star block copolymers in bromoform.

measurements in some of the solvents. The $\langle S^2 \rangle$ value could not be obtained in chlorobenzene in view of extreme distortion of the Zimm and Zimm-Berry plots. The \bar{M}_w and $\langle S^2 \rangle$ values obtained in dioxane are thought to be inaccurate because of the difficulty in maintaining complete dissolution of this sample in this solvent. Except for these two cases, the behavior of 18/23/154 is similar to the previous sample. The \bar{M}_w values are fairly constant and close to the stoichiometric value, thus indicative of a homogeneous sample. As was the case for 18/46/152 the $\langle S^2 \rangle$ values in tetrahydrofuran and toluene (good solvents) are seen to be higher than $\langle S^2 \rangle$ measured in cyclohexane (θ solvent for polystyrene). The value of $\langle S^2 \rangle$ measured in bromoform, which is very close to the true $\langle S^2 \rangle$ of the polyisoprene blocks, is lowest. This again suggests that the polyisoprene component resides in the core of the star block copolymer. Since the results from both 18-arm block copolymer stars suggest a segregated conformation, it was deemed of interest to compare the radii of gyration of the polyisoprene blocks (core) of these 18-arm star block copolymers to that of the homopolyisoprene 18-arm stars of equivalent molecular weights. This should allow some insight into the extent of heterocontacts between the dissimilar segments. Hadjichristidis and Fetters³⁰ have measured the radii of gyration of a series of 18-arm polyisoprene stars in cyclohexane at 35 °C. Since both cyclohexane and bromoform are good solvents for polyisoprene and the intrinsic viscosity values are similar in these solvents,^{18,31} it is assumed that the difference between the radii of gyration measured in cyclohexane and bromoform is negligible. Figure 3 shows the plot of $\langle S^2 \rangle$ vs. \bar{M}_w of the different 18-arm polyisoprene stars and the values of the apparent mean square radii of gyration for 18/46/152 and 18/23/154 measured in bromoform plotted against the weight-average molecular weight values of the respective polyisoprene portions. There it is seen that the polyisoprene center blocks of 18/46/152 and 18/23/154 assume virtually the same dimensions as the corresponding 18-armed homopolyisoprene stars of identical molecular weights. This indicates that there are no mutual interactions between the polystyrene and the polyisoprene blocks and, consequently, the extent of heterocontacts between unlike segments can be considered negligible. Hence it can be concluded that these materials exhibit segregated structures. They may be considered to be vesicle star block copolymers with a polyisoprene core and a polystyrene shell.

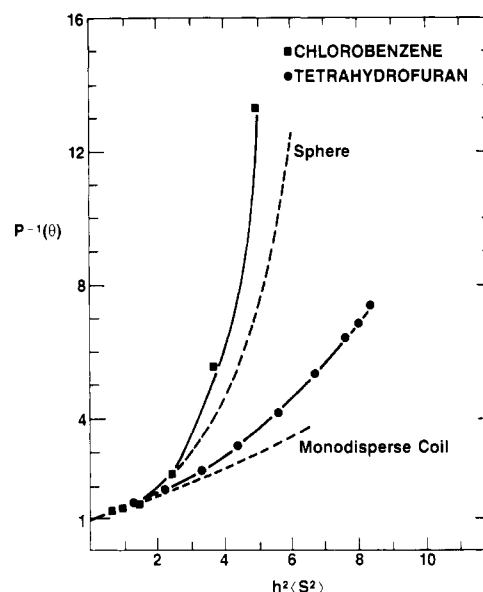


Figure 4. Plot of $P^{-1}(\theta)$ vs. u^2 of the 18/46/152 star block copolymer.

The segregated conformation deduced from the chain dimension studies implies that in chlorobenzene the shape assumed is that of a hollow 18-armed star molecule as predicted by theory.²⁷ Thus, it should be possible to determine the shape of these star block copolymers via an analysis of the particle scattering factor. Unlike the evaluation of the mean square radius of gyration, which can be biased by the scattering points at lower angles, the $P(\theta)$ analysis offers the advantage of considering all the points taken at all angles. This ensures a more faithful interpretation of the experimental data. In special cases, when isorefractive solvents are used, it becomes more difficult as accurate data points at higher angles cannot always be easily obtained. For this reason, the case of bromoform is not treated. Besides, only the lower molecular weight sample, 18/46/152, is suited for this $P(\theta)$ study because, as already pointed out earlier, the higher molecular weight sample 18/23/154 did not permit an accurate determination of both the $\langle S^2 \rangle$ and the $P(\theta)$ in chlorobenzene.

Figure 4 shows the conventional plots of $P^{-1}(\theta)$ vs. u^2 for 18/46/138 measured in chlorobenzene and tetrahydrofuran.³² The curve taken in chlorobenzene shows a much sharper upturn than in tetrahydrofuran at higher u^2 , thus indicating a change in the shape in these solvents. As a point of comparison, Figure 4 also includes the theoretical curves calculated for a monodisperse random coil and of a sphere. It can be seen that the shapes of 18/46/152 both in tetrahydrofuran and in chlorobenzene differ from the shape of either one of the above models. In order to accentuate the difference between the data points taken in tetrahydrofuran and chlorobenzene, it is convenient to resort to the Kratky plot (Figure 5). In a Kratky plot $P(\theta)u^2$ is plotted against u . Figure 5 shows the data of SI 18/46/152 obtained in tetrahydrofuran and chlorobenzene. Figure 5 also includes the theoretical curves, calculated following the method developed by Burchard,²⁸ of a monodisperse 18-arm star, a polydisperse 18-armed star, and a hollow monodisperse 18-arm star. As shown, the experimental curves in tetrahydrofuran and in chlorobenzene closely fit the theoretical curves of the monodisperse 18-armed star and the hollow monodisperse 18-arm star, respectively. It should be recalled that a perfect fit is not expected because the theory was designed for arms following Gaussian statistics (it is unlikely that the arms

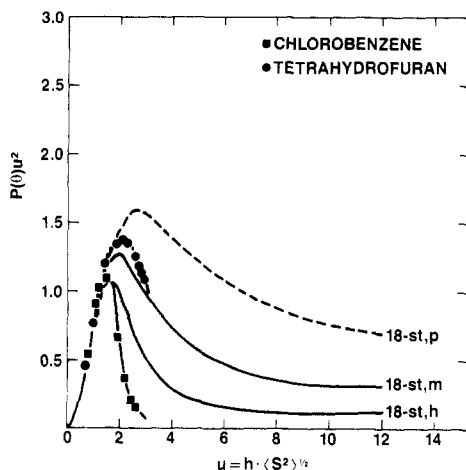


Figure 5. Experimental and theoretical Kratky plots of 18-arm stars (p, polydisperse; m, monodisperse; h, hollow; st, star).

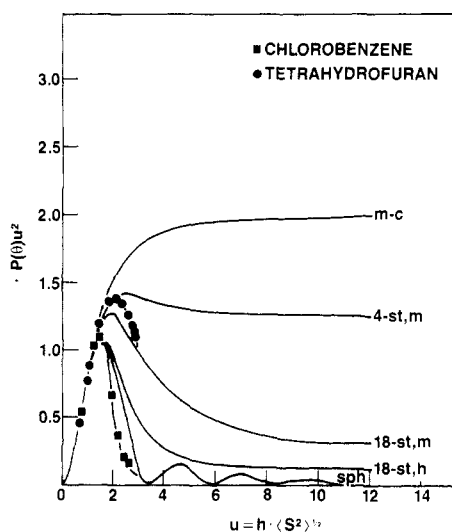


Figure 6. Experimental and theoretical Kratky plots of 18-arm stars (m-c, monodisperse coil; m, monodisperse; st, star; h, hollow; sph, sphere).

of a high-functionality star obey Gaussian statistics in the central region)^{20,21,30,33-39} and for polymers under Θ conditions (chlorobenzene and tetrahydrofuran are good solvents for these star block copolymers). These deviations however are not expected to be significant for very high molecular weight stars and thus the theoretical models still remain good approximations. In chlorobenzene, the experimental points initially fit the shape of an 18-arm hollow star. However, at the theoretical maximum, deviation occurs for the higher u values. Because of the experimental difficulties encountered in obtaining accurate data at high angles in isorefractive solvents it is inappropriate to attempt to rationalize this observation. The experimental points taken in tetrahydrofuran fit more closely the monodisperse 18-arm star than the polydisperse 18-arm star as could have been anticipated given the low dispersity of 18/46/152. These results also favor a segregated conformation. Thus, both the $\langle S^2 \rangle$ and the $P(\theta)$ studies lead to the same conclusion: that the conformation of an 18-armed star block copolymer may be represented by a core and shell model.

To put things into a broader perspective, Figure 6 presents the experimental points in chlorobenzene and tetrahydrofuran and the calculated curves of a monodisperse random coil, a monodisperse 4-arm star, a monodisperse 18-arm star, a hollow monodisperse 18-arm star,

and a solid sphere. As shown, the curve of a 4-arm star comes closer to that of a random coil than a solid sphere. But when the functionality increases, the curve of an 18-arm star comes close to that of a sphere. The theory thus predicts a pronounced change in the shape of a star macromolecule as its functionality increases. Recently Roovers et al.²⁰ have found that high molecular weight 12- and 18-armed star homopolystyrenes behave hydrodynamically almost like hard spheres in dilute solution. From those findings, it is reasonable to expect that the conformation of a high-functionality star block copolymer would differ from that of a low-functionality star block copolymer. Until further results are available, though, the core and shell conformation proposed in the present study should be restricted to the case of high-functionality star block copolymers in dilute solution.

Acknowledgment. This work was supported, in part, by a grant from the National Science Foundation, Polymers Program (Grant DMR-79-08299).

Registry No. Poly(styrene-isoprene) (copolymer), 25038-32-8.

References and Notes

- (1) (a) Present address: Central Research Materials Science and Engineering Products Laboratory, The Dow Chemical Co., Midland, MI 48640. (b) Present address: Division of Chemistry, University of Athens, Athens (10680), Greece. (c) Present address: Corporate Research—Science Laboratories, Exxon Research and Engineering Co., Annandale, NJ 08801.
- (2) Burnett, G. M.; Meares, P.; Patten, C. *Trans. Faraday Soc.* **1962**, *58*, 737.
- (3) Dondos, A.; Froelich, D.; Rempp, P.; Benoit, H. *J. Chim. Phys.* **1967**, *64*, 1307.
- (4) Dondos, A.; Rempp, P.; Benoit, H. *Makromol. Chem.* **1969**, *130*, 233.
- (5) Inagaki, H.; Miyamoto, *Makromol. Chem.* **1965**, *87*, 166.
- (6) Cramond, D. N.; Urwin, J. R. *Eur. Polym. J.* **1969**, *5*, 35.
- (7) Utracki, L. A.; Simha, R.; Fetters, L. J. *J. Polym. Sci., Part A-2* **1968**, *6*, 2051.
- (8) Prud'homme, J.; Bywater, S. *Macromolecules* **1971**, *4*, 543.
- (9) Utiyama, H.; Takenaka, K.; Mizumori, M.; Fukuda, M. *Macromolecules* **1973**, *6*, 28.
- (10) Tanaka, T.; Kotaka, T.; Inagaki, H. *Macromolecules* **1974**, *7*, 311.
- (11) Tanaka, T.; Kotaka, T.; Inagaki, H. *Polym. J. (Tokyo)* **1972**, *3*, 338.
- (12) Han, C. C.; Mozer, B. *Macromolecules* **1977**, *10*, 44.
- (13) Kotaka, T.; Tanaka, T.; Hattori, M.; Inagaki, H. *Macromolecules* **1978**, *11*, 138.
- (14) Tanaka, T.; Kotaka, T.; Inagaki, H. *Macromolecules* **1976**, *9*, 561.
- (15) Tanaka, T.; Kotaka, T.; Inagaki, H. *Macromolecules* **1977**, *10*, 960.
- (16) Bendler, J.; Solc, K.; Gobush, W. *Macromolecules* **1977**, *10*, 635.
- (17) Rahlwes, D.; Roovers, J. E. L.; Bywater, S. *Macromolecules* **1977**, *10*, 604.
- (18) Hadjichristidis, N.; Roovers, J. *J. Polym. Sci., Polym. Phys. Ed.* **1978**, *16*, 851.
- (19) Hadjichristidis, N.; Fetters, L. J. *Macromolecules* **1980**, *13*, 191.
- (20) Roovers, J.; Hadjichristidis, N.; Fetters, L. J. *Macromolecules* **1983**, *16*, 214.
- (21) Huber, K.; Burchard, W.; Fetters, L. J. *Macromolecules* **1984**, *17*, 541.
- (22) Stockmayer, W. H.; Moore, L. D.; Fixman, M.; Epstein, B. N. *J. Polym. Sci.* **1955**, *16*, 517.
- (23) Berry, G. C. *J. Chem. Phys.* **1966**, *44*, 4550. This approach to the handling of light scattering data was adumbrated by Flory in 1953 (Flory, P. J. "Principles of Polymer Chemistry"; Cornell University Press: Ithaca, NY, 1953; p 301).
- (24) Zimm, B.; Stein, R. S.; Doty, P. *Polym. Bull.* **1945**, *1*, 90; Reprinted in: "Light Scattering from Dilute Polymer Solutions"; McIntyre, D., Gornick, F., Eds.; Gordon and Breach: New York, 1964; International Science Review, Series III, p 7.
- (25) Debye, P. *J. Phys. Colloid Chem.* **1947**, *51*, 18.
- (26) Kajiwara, K.; Burchard, W.; Gordon, M. *Brit. Polym. J.* **1970**, *2*, 110.
- (27) Burchard, W. *Macromolecules* **1974**, *7*, 841.
- (28) Burchard, W. *Macromolecules* **1977**, *10*, 919.

- (29) Berry, G. C.; Orofino, T. A. *J. Chem. Phys.* **1964**, *40*, 1614.
 (30) Hadjichristidis, N.; Fetters, L. J., unpublished results.
 (31) Prud'homme, J.; Roovers, J. E. L.; Bywater, S. *Eur. Polym. J.* **1972**, *8*, 901.
 (32) This figure has appeared previously as Figure 12 in Burchard, W.; Kajiwar, K.; Neger, D.; Stockmayer, W. H. *Macromolecules* **1984**, *17*, 222. The polyisoprene segment molecular weight for 18/46/152 given in that reference is incorrect; see

- Table I of this paper for the correct value.
 (33) Mazur, J.; McCrackin, F. *Macromolecules* **1977**, *10*, 326.
 (34) Khokhlov, A. R. *Polymer* **1978**, *19*, 1387.
 (35) Khokhlov, A. R. *Polymer* **1981**, *22*, 447.
 (36) Daoud, M.; Cotton, J. P. *J. Phys. (Les. Ulis, Fr.)* **1982**, *43*, 531.
 (37) Miyake, A.; Freed, K. F. *Macromolecules* **1983**, *16*, 1228.
 (38) Birshtein, T. M.; Zhulina, E. B. *Polymer* **1984**, *25*, 1453.
 (39) Vlahos, C. H.; Kosmas, M. K. *Polymer* **1984**, *25*, 1607.

Neutron Scattering Studies of the Chain Conformation of Poly(methyl methacrylate) Deformed below the Glass Transition Temperature

M. Dettenmaier,^{*,†} A. Maconnachie,[†] J. S. Higgins,[†] H. H. Kausch,[§] and T. Q. Nguyen[§]

Laboratoire de Polymères, Ecole Polytechnique Fédérale de Lausanne, CH-1007 Lausanne, Switzerland, and Department of Chemical Engineering, Imperial College of Science and Technology, London SW7 1BY, U.K. Received November 28, 1984

ABSTRACT: The technique of neutron scattering from mixtures of protonated and deuterated molecules has been used to analyze the conformation of chains in poly(methyl methacrylate) (PMMA) plastically deformed in uniaxial tensile tests. Measurements were conducted on samples that had been stretched to extension ratios of $\alpha = 2.0$ – 2.3 in a temperature range of $T = 60$ – 120 °C. The magnitude of the scattering vector covered a range of $0 < q < 6 \text{ nm}^{-1}$. The results obtained in the low- q range demonstrate that on the scale of the radius of gyration the deformation is approximately affine in the macroscopic strain tensor for long chains ($M_w = 170\,000$ and $250\,000$) but markedly nonaffine for very short ones ($M_w = 6000$). In the intermediate- and high- q range the scattering curve of unstretched PMMA is compared with the scattering curve of stretched PMMA measured perpendicular to the draw axis. The results suggest that pronounced nonaffine modes of plastic deformation are active in regions of less than 2.5 nm .

1. Introduction

Considerable theoretical and technological interest has been focused in the past on the deformation and fracture of glassy polymers. However, the underlying molecular deformation mechanisms are still not very well understood. Most of the information available has been derived from measurements of macroscopic parameters such as stress, strain, and birefringence. The results obtained are generally discussed on the basis of deformation models that start from specific assumptions on the relation between macroscopic and molecular strains (see, e.g., ref 1 and 2). In the affine deformation model it is assumed that these strains are identical on any molecular level, i.e., that the transformation of the distance vector between any pair of molecular segments is affine in the macroscopic strain tensor. In the case of glassy polymers having a nonuniform strain distribution the affine deformation model has been applied to well-defined deformation zones such as shear bands³ and craze fibrils.⁴ The limits of applicability of the affine deformation model are not known at present. In fact, even if this model is valid on sufficiently large molecular scales, it must break down on very small ones because of the existence of intra- and intermolecular hindrances for the conformational rearrangement.

The relation between macroscopic and molecular strains may be established experimentally by using neutron scattering (NS) for the analysis of the conformational re-

arrangement of chain molecules. Most of the experiments have been conducted on amorphous polymers stretched above the glass transition temperature T_g . Very little is known on the chain conformation of amorphous polymers deformed below T_g . Recently, Lefebvre et al.⁵ studied by small-angle neutron scattering (SANS) the chain conformation in shear bands of polystyrene deformed plastically under compression. They reported the existence of non-affine modes of plastic deformation. According to Lefebvre et al.,⁵ the deformation process does not affect the radius of gyration of the molecules within shear bands produced at low strain rates and at higher temperatures. This result has been attributed to the activation of a diffusional mode of plasticity. The isolation of shear bands from the surrounding matrix material and their study by NS cause severe experimental problems. Therefore, measurements on material deformed plastically under different conditions may be useful in examining the affine deformation model. For this reason NS experiments have been conducted on poly(methyl methacrylate) (PMMA), which may be highly deformed plastically in uniaxial tensile tests. The measurements reported in this paper cover a large q range ($0 < q < 6 \text{ nm}^{-1}$) where information is obtained on both the radius of gyration of the molecules and the local arrangement of chain segments.

2. Experimental Section

Sample Preparation. To study the chain conformation of polymers NS measurements are generally conducted on mixtures of unlabeled (protonated) and labeled (deuterated) molecules. The two types of PMMA were prepared by radical polymerization of conventional and deuteriomethyl methacrylate, with benzoyl peroxide and dodecylmercaptan as initiator and transfer agent, respectively. The microtacticity of molecules of PMMA polymerized under these conditions has been analyzed by high-resolution

[†] Present address: Max-Planck-Institut für Polymerforschung, D-6500 Mainz, West Germany.

[§] Laboratoire de Polymères, Ecole Polytechnique Fédérale de Lausanne.

[†] Department of Chemical Engineering, Imperial College of Science and Technology.